3ème conférence Internationale des énergies renouvelables CIER-2015
Proceedings of Engineering and Technology - PET
pp.91-97


# A Robust Fractional Controller Based on Weighted-Mixed Sensitivity Optimization Problem for Permanent Magnet Synchronous Motor

Toufik AMIEUR[1,2], Moussa SEDRAOUI[2], Djamel TAIBI[1], Abdelghani DJEDDI[1], Hanni GUESSOUM[2]

[1] *Department of Electrical Engineering, Kasdi Merbah University, Ouargla, Algeria*
[1]amieur.toufik@univ-ouargla.dz

[2] *Department of Electronic and Telecommunication, 8 May 1945 University, Guelma, Algeria*
[2]msedraoui@gmail.com

***Abstract*— In this paper, a synthesis method of robust Fractional Order PID controller for speed motor of permanent magnet synchronous motor. Space Vector Pulse Width Modulation algorithm and quadrature-axis current loop transfer function based upon nominal plant model of the motor are combined with decoupling technology is established. Parameters of the (FOPID) are obtained which minimizes Integral of Time weighted Absolute Error (ITAE) criterion (Standard H∞ problem) with *Fminimax* optimization algorithm is designed for space vector control model of permanent magnet synchronous motor to improve the speed of tracking performance. The performances obtained are compared with those given by an $H_\infty$ controller using in the frequency domain and in the time.**

***Keywords* — *Fminimax* Optimization Algorithm, Permanent Magnet Synchronous Motor (PMSM), Space Vector Pulse Width Modulation (SVPWM) algorithm, Fractional Order PID (FOPID) controller.**

## I. Introduction

Permanent magnet synchronous motor (PMSM) has received widespread acceptance in industrial servo applications of accurate speed control, because of some of its outstanding features such as superpower density, high torque to current ratio, fast response and better accuracy [1 – 3] . In such applications, the motion controller of PMSM may need to respond relatively swiftly to command changes and to offer enough robustness against the uncertainties of the servo system. However, the control performance of PMSM drive is still affected by uncertainties, which may come internally, or externally, e.g., unpredictable plant parameter variations, external load disturbances, and unmodeled and nonlinear dynamics of the plant. Therefore, in order to enhance the performance of the PMSM drive system, control of the drive system has been a much researched topic that is still ongoing [4–7].

As the motor running in the actual process, there will be some changes in inertia or load changes cases, which likely to affect the system control performance. The servo control itself requires no output overshoot and quickly track the input command, which can hold the state steady and no static error at the same time. Therefore, the motor system needs to have a relatively strong robustness and disturbance rejection for parameter changes. To solve this problem, many researchers have proposed different control schemes, there are fractional order control [8]; adaptive control [9; 10], robust control [11; 12], predictive control [13; 14] and intelligent control [15; 16] are continually incorporated to increase the robustness of the control algorithms.

The robust and adaptive design techniques can confront these uncertainties if process uncertainties are bounded and known prior to the controller design. However the design and analysis procedures are complex and difficult. Also, the process uncertainties are seldom known in advance and are not always bounded [15]. Intelligent control techniques can offer a model free design and administer the process parametric uncertainty and non-linearity but the implementation of these control schemes requires a large number of parameters to be determined prior to the training [17]. For H∞ control, the order of the controller is much higher than that of the plant; hence the high-order H∞ controller is not a welcome option for the most of the engineers. Chattering phenomenon and high heat loss in electrical power circuits are drawbacks for the sliding-mode control. For various PID tuning strategies, the stability of the controlled system should be adequately considered. In references [18–21], a supervisory controller was introduced to guarantee the stability of the closed-loop PID control system. Actually, a success among researchers is the fractional order $PI^{\lambda}D^{\mu}$ [22]. In fact, since the development of the first control approach using the fractional PID controller, different design approaches are proposed [23-25].

This article proposed FOPID space vector model controller of permanent magnet synchronous motor. In the design process of Robust H∞ mixed sensitivity controller, the weighting function parameter selection is generally based on the designer’s experience, using trial and error method [26]. In order to improve the quality control of PMSM system, nonlinear, strong coupling system of PMSM space vector robust controller was designed. The key idea behind the proposed method is formulating the FOPID design problem for PMSM system as a optimization problem with objective function including Integral of Time weighted Absolute Error (ITAE), allowing satisfying some performance specifications such as: a good set point tracking, a satisfactory load disturbance rejection.

## II. Mathematical Model of PMSM Control

The mathematical model of permanent magnet synchronous motor voltage in the *d-q* rotating coordinate system [27]:

$$\begin{cases} U_d = Ri_d + \dfrac{d\phi_d}{dt} - \omega_1\phi_q \\ U_q = Ri_q + \dfrac{d\phi_q}{dt} + \omega_1\phi_q \end{cases} \tag{1}$$

The flux equation can be expressed as:

$$\begin{cases} \phi_d = L_d i_d + \phi \\ \phi_q = L_q i_q \end{cases} \tag{2}$$

The electromagnetic torque can be expressed as:

$$T_e = \frac{3}{2}P\left(\phi_d i_q - \phi_q i_d\right) \tag{3}$$

The dynamic model of motor can be expressed as [27]:

$$\dot{\omega}_M = \frac{1}{J_M}\left(T_e - B\omega_M - T_t\right),\ \omega_1 = P\omega_M \tag{4}$$

Where $U_d$ and $U_q$ are $q$ and $d$ axis voltages; $i_d$ and $i_q$ are $q$ and $d$ axis currents; $R$ is the resistance of the stator windings; $\phi_d$ and $\phi_q$ are $q$ and $d$ axis stator flux; $\phi$ are the permanent magnet flux; $L_d$ and $L_q$ are $q$ and $d$ axis inductances; $p$ is differential operator; $\omega_1$ is electrical angular velocity; $\omega_M$ is mechanical angular velocity; $P$ is number of pole pairs; $T_e$ is electromagnetic torque. $T_t$ is the motor load torque; $J_M$ is the combined inertia of rotor and load; $B$ is the damping coefficient. $i_d = 0$ can be used to achieve current and speed control decoupling. $i_q$ can be regarded as input and $\omega_M$ can be regarded as output. According to Eqs. (1)-(4), we could obtain the current loop control block diagram of permanent magnet synchronous motor, that is shown in **Fig.1** system transfer function is obtained.

$$G(s) = \frac{\omega_M(s)}{I_q(s)} \tag{5}$$

$$\frac{K_T K_p s + K_T K_i}{JLs^3 + \left(BL + J\left(R + K_p K_n\right)\right)s^2 + \left(B\left(R + K_p K_n\right) + K_i K_n J + K_\omega K_{K_T}\right)s + K_i K_n B}$$

Where $K_T = \dfrac{3}{2}P\phi$, $K_{ACR} = K_p + \dfrac{K_i}{s}$, $K_n = R$, $K_\omega = L$

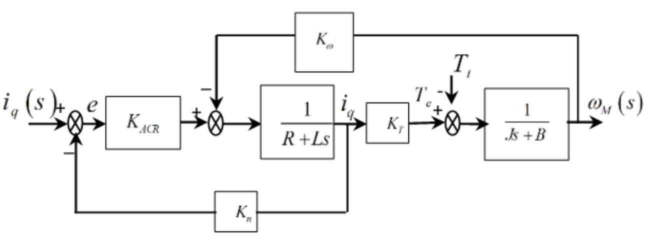

**Fig.1.** The quadrature -axis current loop model of PMSM

Permanent magnet synchronous motor vector control is based on the modular thinking, each control by of the control system is divided into separate sub-module. Including: the coordinate transformation module, the space vector transformation module and the feedback loop coordinate transformation modules. The simulation block diagram of the entire motor control system is shown in **Fig. 2.**

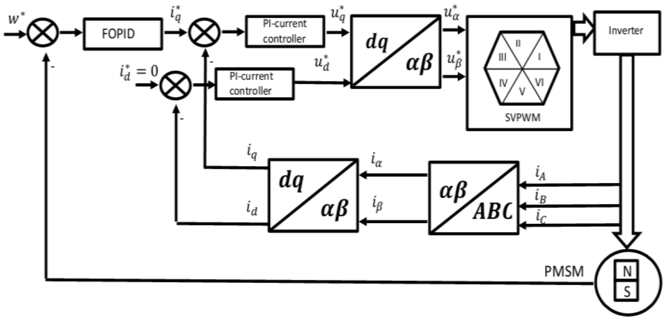


**Fig.2** : The block diagram of PMSM space vector control

In this study, corresponding module parameters are as follows:

**TABLE 1** : PMSM SIMULATION PARAMETRES

| PMSM parametres | Nominal values (p.u) |
|---|---|
| Number of pole pairs, $P$ | 4 |
| Amplitude of flux induced, $\phi$ | $0.175Wb$ |
| Resistance of stator windings, $R$ | $2.8750\Omega$ |
| $d$ and $q$ axes inductances, $L_d$ and $L_q$ | $0.000835H$ |
| Moment of inertia, $J_M$ | $0.008kg/m^2$ |
| Friction coefficient, $B$ | $0.001N.m.s$ |

DC voltage source $U_{dc} = 400V$. In this model, speed loop used PI controller, parameters are as follows: current loop controller of quadrature-axis is $200 + 40/s$ current loop controller of direct axis is $200 + 40/s$.

## III. Fractional Calculus And The Fractional Order PID (FOPID)

### A. Fractional Calculus

Fractional calculus may be explained as the extension of the concept of a derivative operator from integer order $(n)$ to arbitrary order $(v)$ where $(v)$ may be a real value or a complex value or may be a complex valued function $v = v(x,t)$ : $\dfrac{d^n}{dx^n} \rightarrow \dfrac{d^v}{dx^v}$

The most commonly referred definition of fractional derivatives and fractional integrals was given by G. F. B. Riemann and J. Liouville, according to which, the fractional integral of order $(v \succ 0)$ for a function is given by :

$${}_0D_x^{-n} f(x) = \int_c^x \frac{(x-t)^{n-1}}{(n-1)!} f(t)\,dt,\quad n \in N \tag{6}$$

with the condition that $f(x)$ and ${}_0D_x^{-n} f(x)$ are causal functions. For initial conditions to be zero, the Laplace transform of $(D)$ is given by $L\left[{}_0D_x^v\right] = s^v F(s)$ i.e., for zero initial conditions, the system whose dynamic behavior described by differential equations having fractional derivatives re sults in transfer functions with fractional orders of $(s)$ [28]. To simulate fractional order of $(s)$ in MATLAB, this is to be approximated by usual integer order transfer function having an infinite number of poles and zeroes. It is also possible to logicall y approximate it with a finite number of poles and zeros. Oustaloup proposed a method of approximation of a function of the form [29-30]:

$$H(s) = s^{\mu},\ \mu \in R^{+} \tag{7}$$

by a rational function:

$$H(s) = C\prod_{k=-N}^{N} \frac{1+\frac{s}{\omega^{k}}}{1+\frac{s}{\omega'^{k}}} \tag{8}$$

and by applying the following synthesis formulas:

$$\omega_0' = \alpha^{-0.5}\omega_n ; \omega_0 = \alpha^{0.5}\omega_u ; \frac{\omega_{k+1}}{\omega_k} = \frac{\omega_{k+1}}{\omega^{k}} = \alpha n \succ 1 \tag{9}$$

$$\frac{\omega'_{k+1}}{\omega^{k}} = \eta \succ 0 ; \frac{\omega^{k}}{\omega'_{k}} = \alpha \succ 0 ; N = \frac{\log\left(\frac{\omega_N}{\omega_0}\right)}{\log(\alpha\eta)} ; \mu = \frac{\log(\alpha)}{\log(\alpha\eta)}$$

(10)

Where, $\omega_u$ is geometrical mean of the unit gain frequency and the central frequency of a band of frequencies distributed around it. That is,

$$\omega_u = \sqrt{\omega_h \omega_b} \tag{11}$$

Where, $\omega_h$ and $\omega_b$ are the high and low transitional frequencies [31].

### B. Design of $PI^{\lambda}D^{\mu}$ Controller

FOPID controller is an application of fractional calculus theory in PID controller, the differential equation of it in time domain is described by [32]:

$$u(t) = Kp * e(t) + Ki * D_i^{-\lambda} e(t) + Kd * D_i^{\mu} e(t) \tag{12}$$

The continuous transfer function of the fraction order PID controller is obtained through the Laplace transform is shown as follows [32]:

$$K(s,\underline{x}) = Kp + \frac{Ki}{s^{\lambda}} + Kd * s^{\mu} \tag{13}$$

It is obvious that the FOPID controller nor only contains conventional proportional, integral and derivative gains $(Kp, Ki, Kd)$, but also owns additional integration and differentiation orders $(\lambda, \mu)$, which is adjustable parameters that gives more possibility to realize the desired control performance. While $\lambda = 1$ and $\mu = 1$, the FOPID controller structure is reduced to the classical PID controller. Yields also the following design parameter vector: $\underline{x} = [Kp, Ki, Kd, \lambda, \mu]$

## IV. The $H_\infty$ Design Of Controllers

### A. Robust Control

Robust mixed sensitivity control model of $G(s)$ is shown in **Fig.3**, the sensitivity function $S$, the input sensitivity function $R$ and complementary sensitivity functions $T$ respectively are:

$$\begin{cases} S(s) = (I + K(s)G(S))^{-1} \\ R(s) = (I + K(s)G(S))^{-1} K(s) \\ T(s) = (I + K(s)G(S))^{-1} K(s)G(s) \end{cases} \tag{14}$$

In the figure, $G(s)$ the transfer functions of the nominal plant; $K(s)$ is the output feedback controller; $u, y, r$ respectively, as a control signal, the observation signal, the external input. The choice of the weighting function should be compromise because there are limitations of $S + T = I$ in the same frequency band. In addition, $S, T$ and $R$ should satisfy robust control theorems. Internal system is stable and satisfies the desired performance so the controller design problem is transformed into the suppression problem of the H∞ norm $\xi$.

$P = \|T_{zw}\|_\infty = \left\| \begin{matrix} W_S S \\ W_R R \\ W_T T \end{matrix} \right\|_\infty \le \xi$, The general value of $\xi$ is 1.

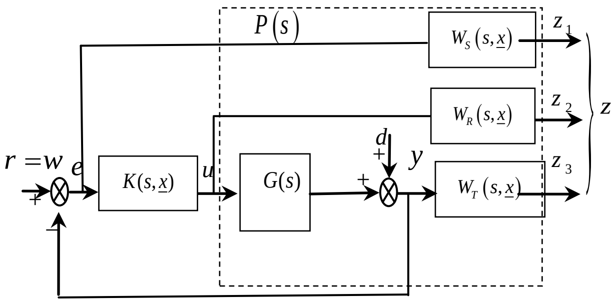


**Fig. 3.** $H_\infty$ mixed sensitivity configuration**.**

### B. Design Methodology of the Weighting Functions

As aforementioned, the H∞ control design using the mixed-sensitivity configuration requires three weighting functions, which reflect the various performance requirements of the system. $W_S(s)$, $W_T(s)$ and $W_R(s)$ are the tracking performance and stability weighting functions, respectively. The very general guidelines for weighting functions choice (15-17) were proposed in [33-36] and were used in this paper, though were not strictly followed:

$$W_S(s) = \left( \frac{\frac{s}{\sqrt{M_S}} + \omega_B^*}{s + \omega_B^* A_S} \right) \tag{15}$$

$$W_T(s) = \left( \frac{\frac{s}{\omega_{BT}^*} + \frac{1}{\sqrt{M_T}}}{\frac{A_T s}{\omega_{BT}^*} + 1} \right) \tag{16}$$

$$W_R(s) = K \tag{17}$$

Where $M_S$ and $M_T$ are high frequency gains, $A_S$ and $A_T$ are low frequency gains, $\omega_B^*$ and $\omega_{BT}^*$ determine crossover frequency. The desirable $W_S(s)$ has low-pass characteristics that ensure the tracking performance and disturbance attenuation. The maximum singular value of the sensitivity transfer function $S(s,x)$ should be less than the maximum singular value of $W_S^{-1}(s)$ in all frequency domains:

$$\bar{\sigma}\left[S(j\omega,x)\right] \prec \bar{\sigma}\left[W_S^{-1}(j\omega)\right] \quad (18)$$

- The weighting functions $W_T(s)$ restricts the robust boundary of the system. The maximum singular value of complementary sensitivity transfer function $T(s,x)$ should be less than the maximum singular value of $W_T^{-1}(s)$ in all frequency domains:

$$\bar{\sigma}\left[T(j\omega,x)\right] \prec \bar{\sigma}\left[W_T^{-1}(j\omega)\right] \quad (19)$$

Moreover, $W_S(s)$ and $W_T(s)$ need to satisfy the following inequality constraint:

$$\bar{\sigma}\left[W_S^{-1}(j\omega)\right] + \bar{\sigma}\left[W_T^{-1}(j\omega)\right] \geq 1 \quad (20)$$

Taking these performance indicators of inequality constraints, the objective function can be obtained:

$$\phi_6 = \int_{t_0}^{t_f} t\left|e(t,\underline{x})\right|dt$$

Where: $e(t,\underline{x}) = \omega_{ref}(t) - \omega(t,\underline{x})$, $\underline{x}_{\min} \leq \underline{x} \leq \underline{x}_{\max}$.

## V. Simulation Results

Under the MATLAB/Simulink environment, we use the established space vector control of PMSM system combines the design of robustness mixed sensitivity controller simulation. We use the established space vector control system of PMSM combining with the design of robust mixed sensitivity controller to simulate. The **Fig.4** compares between the maximal singular values of the inverse weighting matrices $1/W_S(s)$ and sensitivity matrices $S(s,\underline{x})$ .The **Fig.5** compares between the maximal singular values of the inverse weighting matrices $1/W_T(s)$ and complementary sensitivity matrices $T(s,\underline{x})$.

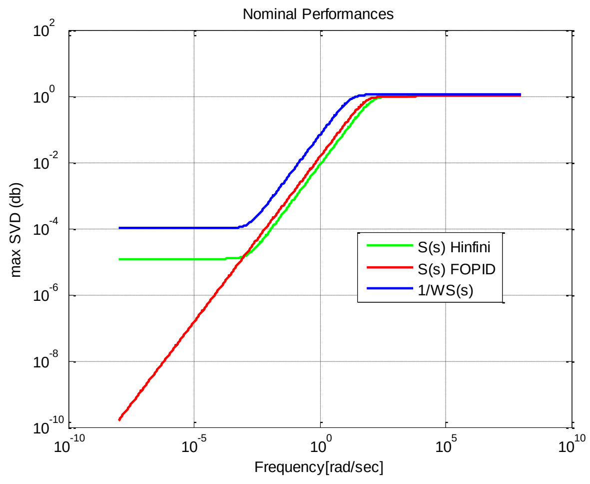


**Fig.4.** Comparison between maximal singular values of $1/W_S(s)$ and $S(s)$

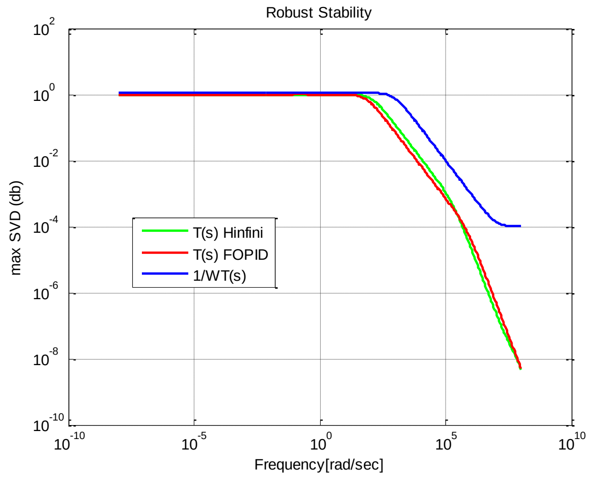


**Fig.5.** Comparison between maximal singular values of $1/W_T(s)$ and $T(s)$

To confirm these results in the time domain, the blocks of the Simulink Matlab® are used in order to loop-shape the perturbed system by a FOPID and robustified $H_\infty$ controllers.

**Fig.6.** is the response curve of the system that a given initial speed of 400 r/min to 700 r/min in 0.005s.

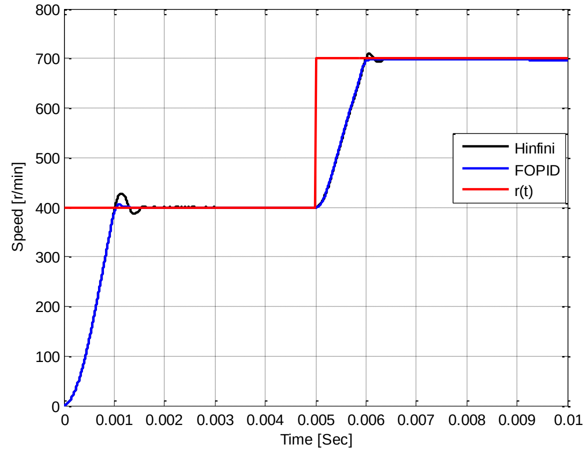

**Fig.6.** Speed

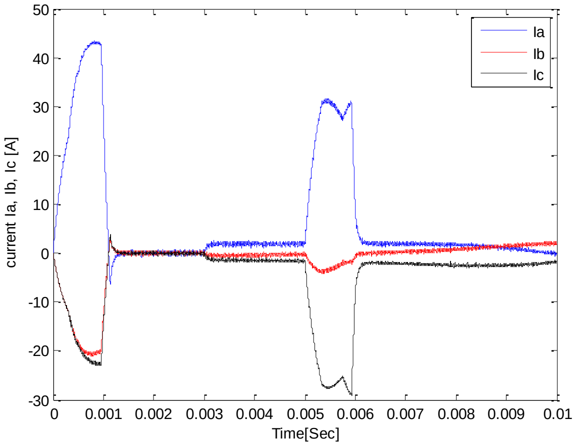


**Fig.7.** Three-phase current.

The load torque at $t = 0.003$sec mutated to $T_t = 2N.m$ is shown in **Fig.8.**

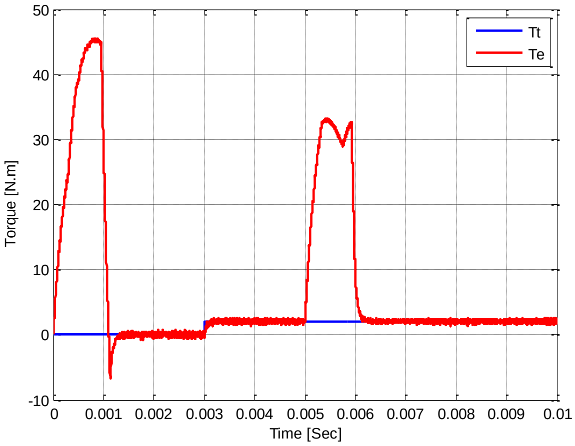


**Fig.8.** Torque.

## VI. CONCLUSION

This paper established a space vector control model of permanent magnet synchronous motor; the robust FOPID controller is designed according to the transfer function of quadrature-axis current loop. In this work the *Fminimax* algorithm has been utilized to find the optimal parameters of FOPID controller which minimizing the (ITAE). The system with FOPID controller exhibit good frequency and time domain response as compared with the H∞ controller. The simulation results show that the control system has an excellent dynamic performance, it can be effectively suppressed the adverse effects by load disturbances. The designed controller ensures the robust performance of PMSM space-vector system.

## REFERENCES


[1] Luo Y., Chen Y. and Pi Y. Cogging effect minimization in PMSM position servo system using dual high-order periodic adaptive learning compensation. *ISA Transactions;* 2010; 49( 4), pp. 479 – 88.

[2] Liu, H., and Li S. Speed control for PMSM servo system using predictive functional control and extended state observer. *IEEE Transactions on Industrial Electronics;* 2012; 59(2), pp: 1171 – 83.

[3] Zhang B, Pi Y, Luo Y. Fractional order sliding-mode control based on parameters auto-tuning for velocity control of permanent magnet synchronous motor. *ISA Transactions;* 2012; 51(5), pp. 649 – 56.

[4] Mohamed YA-RI. Adaptive self-tuning speed control for PMSM with dead-time. *IEEE Transactions on Energy Conversion*; 2006; 21(4): pp. 855 – 862.

[5] Sepe R, Lang J. Real-time observer-based (adaptive) control of a permanent magnet synchronous motor without mechanical sensors. *IEEE Transactions on Industry Applications;* 1992; 28(6), pp.1345 –1352.

[6] Li S, Gu H. Fuzzy adaptive internal model control schemes for pmsm speed-regulation system. *IEEE Transactions on Industrial Informatics;* 2012;8(4), 76 7– 79.

[7] Zhang X, Sun L, Zhao K, Sun L. Nonlinear speed control for PMSM system using sliding-mode control and disturbance compensation techniques. *IEEE Transactions on Power Electronics;* 2013;28(3):1358– 65.

[8] Zhang, B. T., & Pi, Y. Robust fractional order proportion-plus-differential controller based on fuzzy inference for permanent magnet synchronous motor. *IET Control Theory Applications*; 2012; 6(6), pp. 829–837

[9] Abdel-Rady, Y., & Mohamed, I. Adaptive self-tuning speed control for permanent-magnet synchronous motor drive with dead time. *IEEE Transactions on Energy Conversion*; 2006; 21(4), pp. 855–862.

[10] Li, S. H., & Liu, Z. G. Adaptive speed control for permanent magnet synchronous motor system with variations of load inertia. *IEEE Transactions on Industrial Electronics*;2009; 56(8), pp. 3050–3059.

[11] Ghafari-Kashani, A. R., Faiz, J., and Yazdanpanah, M. J. Integration of nonlinear H1 and sliding mode control techniques for motion control of a permanent magnet synchronous motor. *IET Electrical Power Applications*, ;2010;4(4), pp. 267–280.

[12] Zhang, X., Sun, L., Zhao, K., and Sun, L. Nonlinear speed control for PMSM system using sliding-mode control and disturbance compensation techniques. *IEEE Transactions on Power Electronics;* (2013); 28(3), pp. 1358–1365.

[13] Preindl, M., & Bolognani, S. Model predictive direct speed control with finite control set of PMSM drive systems. *IEEE Transactions on Power Electronics*; 2013a; 28(2), pp. 1007–1015.

[14] Preindl, M., & Bolognani, S. Model predictive direct torque control with finite control set for PMSM drive systems, Part 2: Field weakening operation. *IEEE Transactions on Industrial Informatics*; 2013b; 9(2), pp. 648–657.

[15] El-Sousy, F. F. M. Intelligent optimal recurrent wavelet Elman neural network control system for permanent-magnet synchronous motor servo drive. *IEEE Transactions on Industrial Informatics;* 2013; 9(4), pp.1986–2003.

[16] Li, S., & Gu, H. Fuzzy adaptive internal model control schemes for PMSM speed-regulation system. *IEEE Transactions on Industrial Informatics*; 2012; 8(4), 767–779.

[17] Uddin, M. N., & Wen, H. Development of a self-tuned neuro-fuzzy controller for induction motor drives. *IEEE Transactions on Industry Applications;* 2007; 43(4), pp. 1108–1116.

[18] Chang W. D., Yan J. J. Adaptive robust PID controller design based on a sliding mode for uncertain chaotic systems. Chaos, Solitons and Fractals; 2005; 26(1), pp. 167–75.

[19] Kansha Y, Jia L, Chiu M. S. Self-tuning PID controllers based on the Lyapunov approach. *Chemical Engineering Science* 2008; 63(10), pp.2732 – 2740.

[20] Hsu C.F., Lee B.K. FPGA-based adaptive PID control of a DC motor driver via sliding-mode approach. *Expert Systems with Applications;* 2011; 38(9), pp. 11866 – 11872.

[21] Vikas K., Prerna G. and A.P. Mittal. ANN based self-tuned PID like adaptive controller design for high performance PMSM position control. *Expert Systems with Applications;* 2014; 41, pp. 7995–8002.

[22] Podlubny, I. Fractional-order systems and $PI^{\lambda}D^{\upsilon}$ controller. *IEEE Transaction on automatic Control*, 1999.Vol. 44, pp. 208–214.

[23] Monje, C., Vinagre, B., Feliu, V., and Chen, Y. Tuning and auto-tuning of fractional order controllers for industry applications. *Control Engineering Practice*; 2008; Vol. 16, No. 7, pp. 798–812.

[24] Petras, I. Fractional-order feedback control of a dc motor. *Journal of Electical Engineering*; 2009; vol. 21, pp. 3182–3187.

[25] Liang, T., Chen, J., and Lei, C. Algorithm of robust stability region for interval plant with time delay using fractional order $PI^{\lambda}D^{\upsilon}$ controller. *Commun Nonlineair Sci Numer Simulat*; 2011; Vol. 17, pp. 979–991.

[26] ZANG Huai-quan, WANG Yuan-yuan. Robust H∞ control for electric power steering based on genetic algorithm. *Control Theory & Applications*; 2012; 29(4), pp. 544-548.

[27] Hany M. H., Torque ripple minimization of permanent magnet synchronous motor using digital observer controller, *Energy Conversion and Management, Elsevier*; 2010; Vol. 51, pp. 98–104.

[28] Miller, K. S. and Ross, B. An Introduction to the Fractional Calculus and Fractional Differential Equations. *New York. Conference on Evolutionary Computation, John Wiley & Sons. Inc;* 1993; pp. 69–73.

[29] Oustaloup, A., Levron, F., Mathieu, B., and Nanot, F. Frequency-band complex non integer differentiator: characterization and synthesis. *IEEE Trans. Circ. Sys.: Fundamental Theory and Applications*; 2000; Vol. **47**, pp. 25–39.

[30] Gao, Zhe, Liao and Xiaozhong. Improved Oustaloup approximation of fractional order operator using adaptive chaotic particle swarm optimization. *Journal of System Engineering Electronics*; 2012; vol. 23, No. 1, pp. 145-153.

[31] Bensafia, Y. and Ladaci, S. Adaptive control with fractional order reference model. *International journal of sciences and techniques of automatic control & computer engineering*; 2011; Vol. 5, pp.1614-1623.

[32] Zhihuan Chen, Xiaohui Yuan, Bin Ji, Pengtao Wang, Hao Tian, Design of a fractional order PID controller for hydraulic turbine regulating system using chaotic non-dominated sorting genetic algorithm II, *Energy Conversion and Management;* 2014; 84, pp. 390–404.

[33] Beaven R.W., Wright M.T., Seaward D.R. Weighting Function Selection in the $H_1$ Design Process. *Control Eng. Practice*; 1996; vol.4, No.5, pp. 625–633.

[34] Oloomi, H., and Shafai, B. Weight selection in mixed sensitivity robust control for improving the sinusoidal tracking performance. *In Decision Cont. Proce. 42nd IEEE Conf.**1***; 2003; pp. 300-305.

[35] Ortega, M.G, and Rubio, F.R. Systematic design of weighting matrices for the $H_\infty$ mixed sensitivity problem. *J. process cont*; 2004; Vol. **14**, pp. 89-98.

[36] Zhang, N., Gu, W., Yu, H. and Liu, W. Application of Coordinated SOFC and SMES Robust Control for Stabilizing Tie-Line Power. *Energies*; 2013; Vol. 6, pp. 1902-1917.